Journal of
Applied Crystallography
ISSN 0021-8898

Received 30 March 2005
Accepted 15 July 2005

A comparison of methods for modeling the effect of axial divergence in powder diffraction

E. Prince and B. H. Toby*

NIST Center for Neutron Research, National Institute of Standards and Technology, Gaithersburg, Maryland 20899, USA. Correspondence e-mail: brian.toby@nist.gov

The Edgeworth series model for the modification of diffraction peak shapes because of axial divergence is compared with the peak shapes computed by a numerical convolution method that is computationally slow. It is shown that if the width of an approximately Gaussian instrumental peak shape is comparable with the width of the modifying function, a condition that is generally satisfied in fixed-wavelength neutron diffraction and in many laboratory X-ray diffraction instruments, but not with synchrotron X-ray instruments, the Edgeworth model is nearly identical to the convolution model, while the computation is much simpler.

1. Introduction

The cornerstone of full-pattern fitting methods, such as the Rietveld technique (Rietveld, 1969), rests on the ability to fit peak profiles seen in powder diffraction experiments. One of the more difficult aspects of modeling powder diffraction profiles is caused by so-called 'low-angle peak asymmetry', which arises both at very small and very large diffraction angles due to axial divergence.

The mechanism that gives rise to this broadening can be readily understood. When a narrow beam of monochromatic radiation with wavelength λ is incident on a polycrystalline sample, the radiation diffracted from lattice planes with lattice spacing d lies on a circular cone with semiangle 2θ, where θ is given by Bragg's law, $\sin\theta = \lambda/2d$. If this cone were intercepted by a flat film tangent to a circle centered at the sample at angle 2θ, the trace of the cone would be an ellipse with one focus where the incident beam intercepts the plane of the film. A conventional fixed-wavelength diffractometer samples a short segment of the ellipse through a rectangular slit whose long dimension is tangential to the ellipse and whose short dimension is short compared with the instrumental width of the diffracted beam. Although similar results are found for other diffraction geometries, in the following discussion we shall assume that the sample is a cylinder whose axis is perpendicular to the incident beam, and that the detector slit is scanned in a plane perpendicular to the sample axis.

As the detector slit is scanned across the diffraction cone, the intensity peak has a shape given by the convolution of the detector's resolution function with the elliptical trace of the diffraction cone. The elliptical trace has several effects. For values of 2θ less than 90°, the centroid of the peak is shifted toward a lower angle, the peak is broadened, and the peak is asymmetrical, with a tail extending toward lower angles. For diffraction values of 2θ greater than 90°, the effect is in the opposite direction. The effect is greatest closest to 0 and 180°, where the curvature of the diffraction cone is greatest.

In the first 25 years of full-pattern fitting, broadening arising from low-angle asymmetry was treated simplistically and the peak shift was generally ignored. Failure to treat the peak shift introduces a small bias into the refined lattice constants and the zero point, while inaccuracies in broadening are absorbed into the parameters describing the peak widths (Caglioti *et al.*, 1958). In this initial period there were several approaches to modeling the asymmetry effect. Rietveld (1969) introduced a 'semiempirical' function, and Howard (1982) tried one that was based on several overlapping Gaussian functions. Another approach utilized differing profile parameters below the peak maximum *versus* above the maximum, thus 'splitting' the peak. While this could be done with many functions, it was most commonly done with Pearson VII type functions (see *e.g.* Brown & Edmonds, 1980). All of these procedures present problems with the normalization of the integrated intensities of the peaks in different parts of the pattern. Prince (1983) first analyzed the problem geometrically using a cumulant expansion of the Fourier transform of the peak shape function, then representing the actual function by a truncated Edgeworth series (Prince, 2004). This procedure solves the normalization problem, but is only possible when the underlying instrumental resolution function is close to Gaussian, a condition that is usually satisfied in fixed-wavelength neutron diffraction, but not with synchrotron radiation.

A direct approach to the convolution problem was first proposed by van Laar & Yelon (1984) and was implemented both by Eddy *et al.* (1986) and by Finger *et al.* (1994). Software developed by Finger *et al.* (referred to as FCJ hereinafter) was widely distributed and has achieved widespread acceptance. The FCJ approach, which uses numerical evaluation of the integrals involved, is mathematically rigorous and independent of the instrumental peak shape, but is computationally

extremely slow, even with modern computers. The FCJ model has two seemingly non-adjustable parameters, describing the ratio of the sample height and the detector aperture height to the diffractometer radius. However, the derivation assumes that the incident beam is parallel in the axial direction. To account for the actual divergence, particularly when focusing monochromators are employed, requires the use of an effective sample height, which is determined by refinement.

Prince (1983) gives expressions for the cumulants of the peak shape function in terms of the moments of the axial resolution function, and evaluates them in the cases where that function is Gaussian and rectangular (which corresponds to a sample whose axial extent is small compared with the length of the slit). In that work, the asymmetry parameter was treated as an adjustable parameter to be refined. In this paper, we extend the Edgeworth series approach to fourth cumulant terms, adopt the parameterization of FCJ, and compare the Edgeworth series result with the FCJ results, calculated in the case where the sample length and detector slit length are identical, which implies a triangular axial resolution function. Peak shapes are calculated under various conditions of experimental resolution and sample and slit dimensions. We demonstrate that this approach can produce nearly identical results to the FCJ results, with dramatic computational simplification, except in cases where extremely high resolution is present at very low diffraction angles. Thus, the Edgeworth series approximation is appropriate for neutron diffraction, many laboratory X-ray diffraction instruments, but not for all synchrotron applications.

2. The Edgeworth model

Consider a diffractometer with its axis vertical and a slit of half height H located at radius R from a sample with half height S. Prince (1983) showed that the moments, $\langle\delta^n\rangle$, of the function that modifies the peak shapes because of the curvature of the elliptical trace of the diffraction cone could be represented by expressions that reduce to

$$\langle\delta^n\rangle = (-1)^n[\langle z^{2n}\rangle/(2R^2\tan 2\theta)^n], \tag{1}$$

where z is the difference in height between a point in the sample and a point in the slit. Here

$$\langle z^{2n}\rangle = \int z^{2n}\rho(z)\,\mathrm{d}z, \tag{2}$$

where $\rho(z)$ is the vertical resolution function. FCJ consider the realistic case where H and S have similar magnitudes, and $\rho(z)$ is trapezoidal, with the short edge equal to $2(H-S)$ and the long edge equal to $2(H+S)$. If we let $A = H - S$ and $B = H + S$, then

$$\langle z^{2n}\rangle = \frac{2}{A+B}\left[\int_0^A z^{2n}\mathrm{d}z + \int_A^B z^{2n}\left(\frac{B-z}{B-A}\right)\mathrm{d}z\right], \tag{3a}$$

which evaluates to

$$\langle z^{2n}\rangle = \frac{B^{2n+2} - A^{2n+2}}{(n+1)(2n+1)(B^2-A^2)}. \tag{3b}$$

Then

$$\langle z^2\rangle = \frac{B^2+A^2}{6}, \tag{4a}$$

$$\langle z^4\rangle = \frac{B^4+B^2A^2+A^4}{15}, \tag{4b}$$

$$\langle z^6\rangle = \frac{B^6+B^4A^2+B^2A^4+A^6}{28} \tag{4c}$$

and

$$\langle z^8\rangle = \frac{B^8+B^6A^2+B^4A^4+B^2A^6+A^8}{45}. \tag{4d}$$

A diffraction peak is represented by a density function, $P(2\theta)$, normalized so that the integral over the peak is equal to 1, with its centroid at $2\theta = 2\theta_\mathrm{B} + \langle\delta\rangle$, where θ_B is the Bragg angle calculated from the wavelength and the unit-cell constants. Its broadened width can be represented by a standard deviation, σ_b, given by $\sigma_\mathrm{b} = (\sigma_\mathrm{i}^2 + \langle\delta^2\rangle - \langle\delta\rangle^2)^{1/2}$, where σ_i^2 is the variance of the instrumental resolution function, the limiting peak shape function as (H/R) approaches zero. [The full width at half-maximum (FWHM) of a Gaussian peak is $2(2\ln 2)^{1/2}\sigma$.] These expressions are exact, regardless of the shape of the instrumental resolution function, provided that its first two moments exist.

If the experimental resolution function is approximately Gaussian, the effect of the diffraction cone may be represented by an Edgeworth series (Prince, 2004). First, make the linear transformation $x = (2\theta + \langle\delta\rangle)/\sigma_\mathrm{b}$, remembering that $\langle\delta\rangle$ is negative. Then the function

$$\gamma(x) = \frac{1}{(2\pi)^{1/2}}\exp\left(-\frac{x^2}{2}\right) \tag{5}$$

is a normalized Gaussian with mean zero and variance one. A function that has the same first four moments as the modified peak shape function is

$$P(x) = \gamma(x)\left[1 + \frac{{}^3\kappa}{6\sigma_\mathrm{b}^3}\mathrm{H}_3(x) + \frac{{}^4\kappa}{24\sigma_\mathrm{b}^4}\mathrm{H}_4(x)\right], \tag{6}$$

where

$${}^3\kappa = \langle\delta^3\rangle - 3\langle\delta^2\rangle\langle\delta\rangle + 2\langle\delta\rangle^3 \tag{7a}$$

and

$${}^4\kappa = \langle\delta^4\rangle - 4\langle\delta^3\rangle\langle\delta\rangle - 3\langle\delta^2\rangle^2 + 12\langle\delta^2\rangle\langle\delta\rangle^2 - 6\langle\delta\rangle^4 \tag{7b}$$

are the third and fourth cumulants of the modifying function, respectively.

$$\mathrm{H}_3(x) = x^3 - 3x \tag{8a}$$

and

$$\mathrm{H}_4(x) = x^4 - 6x^2 + 3 \tag{8b}$$

are the third- and fourth-degree Hermite polynomials, respectively. Because of the orthogonality properties of the

Hermite polynomials, this function is also normalized. It is not, however, guaranteed to be everywhere positive, but any negative regions will be well down in the high-angle tail, and small compared with the statistical fluctuations in the background.

The expressions for $\langle z^{2n}\rangle$ given in equations (4*a*) to (4*d*) are symmetric with respect to interchanges of A and B, and, because A and B always occur as even powers, they are also symmetric with respect to interchanges of H and S. Because H is a constant for a particular diffractometer configuration, we choose to treat the effective sample height as the refinable variable. To do this it is necessary to determine the partial derivative of the peak shape function [equation (6)] with respect to S/R. The straightforward but tedious mathematics is given as supplementary material.[1]

3. Comparison of Edgeworth model with numerical convolution

In order to compare the Edgeworth model with the FCJ numerical convolution procedure we have written a computer program that calculates peak shapes under various conditions of diffractometer geometry and resolution according to the Edgeworth model and the numerical model as implemented in the subroutine *PROFVAL*, supplied by L. W. Finger. The source code for this program is included in the supplementary material. We also supply as supplementary material source code for the partial derivatives of the peak shape function with respect to the refinable parameters.[1]

Fig. 1 shows the calculated peak shape curves for the Edgeworth model and for the FCJ method, compared with an unmodified Gaussian curve with a FWHM of 0.25°, where $S/R = H/R = 0.03$, and $2\theta = 10.0°$. These conditions are typical of those found at the powder diffractometer BT-1 at the NIST Center for Neutron Research. The curves are virtually identical. Because the peaks in a typical synchrotron powder diffraction pattern are much sharper, the peak shape will be dominated by the shape of the modifying function, which is not at all like a Gaussian. To get some idea of the limits of applicability of the Edgeworth model, Fig. 2 shows the comparable curves for the same conditions as in Fig. 1, except that the FWHM of the unmodified Gaussian is 0.10°. It is evident that at this level of resolution the Edgeworth model is inadequate.

To quantify this comparison, we define a figure of merit by

$$M = \left[\sum (I_{\rm E} - I_{\rm F})^2 / \sum I_{\rm F}^2\right]^{1/2}, \qquad (9)$$

where $I_{\rm E}$ and $I_{\rm F}$ are the values of the peak shape function as calculated from the Edgeworth model and the FCJ procedure, respectively, and the sum is taken over the region in which either function is significantly different from zero. Consider the case (the worst case) where H and S are equal. Then $A = 0$, $B = 2H$, and equation (3*b*) reduces to

$$\langle z^{2n}\rangle = \frac{(2H)^{2n}}{(n+1)(2n+1)}. \qquad (10)$$

Then the moments of the distorting function become

$$\langle \delta^n\rangle = \left[-\frac{2H^2\cot 2\theta}{(n+1)(2n+1)R^2}\right]^n. \qquad (11)$$

The third and fourth cumulant coefficients in the Edgeworth series expansion are therefore proportional to $\cot^3 2\theta$ and $\cot^4 2\theta$, respectively, and decrease rapidly with increasing values of 2θ. The upper curve in Fig. 3 shows M as a function of 2θ for $H/R = S/R = 0.03$, and FWHM = 0.10°. For values of M less than about 0.05, the curves are virtually indistinguishable.

If H is reduced while holding S fixed, thus making the detector slit height smaller than the sample height, the higher cumulant coefficients are also reduced rapidly. Note that this

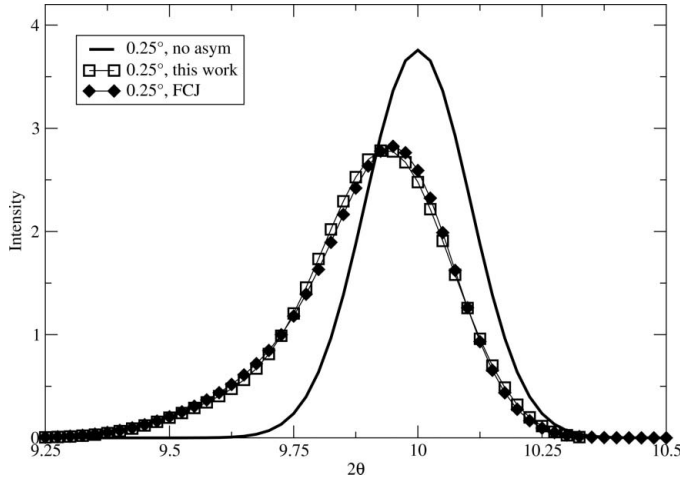

Figure 1
Curves of peak shapes according to the Edgeworth model and the numerical convolution model, with $S/R = H/R = 0.03$, $2\theta = 10.0°$, and the full width at half-maximum (FWHM) of the undistorted peak equal to 0.25°.

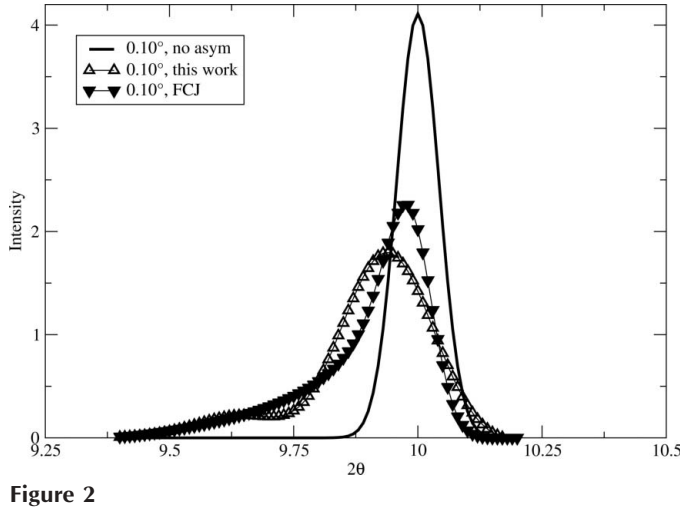

Figure 2
Curves of the Edgeworth model and the numerical convolution model with $S/R = H/R = 0.03$, $2\theta = 10.0°$, and FWHM of the unmodified Gaussian = 0.10°.

[1] Supplementary data are available from the IUCr electronic archives (Reference: HX5030). Services for accessing these data are described at the back of the journal.

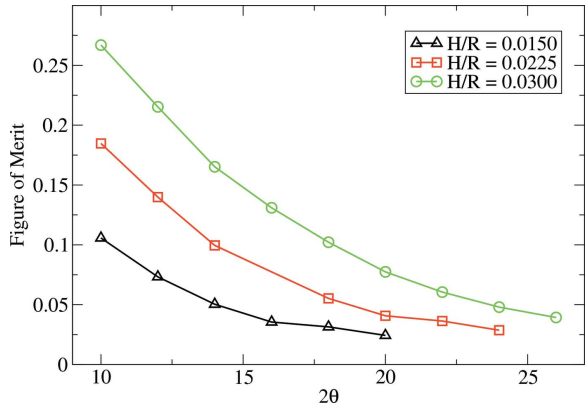

Figure 3
Values of the figure of merit, M (see text), as a function of 2θ for a Gaussian peak with FWHM = 0.10°, and several values of H/R. For M less than 0.05, the curves of the Edgeworth model and the FCJ model are virtually indistinguishable.

causes a reduction in detector sensitivity, but this reduction is linear, while the Lorentz factor is proportional to $1/\sin(2\theta)$ and increases rapidly at low angles, compensating for the reduced detector sensitivity. The middle and lower curves in Fig. 3 show M for $H/R = 0.0225$ and $H/R = 0.015$, respectively. It is obviously advantageous to collect data using different axial divergences in different angle ranges. The multidetector neutron powder diffractometer at the NIST Center for Neutron Research incorporates smaller slit heights in the lowest angle detectors to take advantage of this effect.

4. Conclusions

This work has demonstrated that the Edgeworth model can be parameterized in the same fashion as the FCJ model. The two models agree very well except when low-angle peaks are very narrow. Cases where the Edgeworth model fails can be detected easily by comparison of the standard deviation of the instrumental peak, σ_i, with that of the modifying function, σ_m. However, where the models are in agreement, the Edgeworth approach is computationally much simpler. We plan to implement the Edgeworth model within the *GSAS* suite of software (Larson & Von Dreele, 2000).

References

Brown, A. & Edmonds, J. W. (1980). *Adv. X-ray Anal.* **23**, 361–374.
Caglioti, G., Paoletti, A. & Ricci, F. P. (1958). *Nucl. Instrum.* **3**, 223–228.
Eddy, M. M., Cheetham, A. K. & David, W. I. F. (1986). *Zeolites*, **6**, 449–454.
Finger, L. W., Cox, D. E. & Jephcoat, A. P. (1994). *J. Appl. Cryst.* **27**, 892–900.
Howard, C. J. (1982). *J. Appl. Cryst.* **15**, 615–620.
Laar, B. van & Yelon, W. B. (1984). *J. Appl. Cryst.* **17**, 47–54.
Larson, A. C. & Von Dreele, R. B. (2000). *General Structure Analysis System* (*GSAS*), Report LAUR 86-748, Los Alamos National Laboratory, USA.
Prince, E. (1983). *J. Appl. Cryst.* **16**, 508–511.
Prince, E. (2004). *Mathematical Techniques in Crystallography and Materials Science*, 3rd ed., pp. 134–139. New York: Springer Verlag.
Rietveld, H. M. (1969). *J. Appl. Cryst.* **2**, 65–71.